

An Explicit Multi-Level Time-Step Algorithm to Model the Propagation of Interacting Acoustic-Elastic Waves Using Finite Element/Finite Difference Coupled Procedures

D. Soares Jr.^{1,2}, W.J. Mansur¹ and D.L. Lima³

Abstract: The present paper discussion is concerned with the development of robust and efficient algorithms to model propagation of interacting acoustic and elastic waves. The paper considers acoustic-elastic, acoustic-acoustic and elastic-elastic partitioned analyses of coupled systems; however, the focus here is the acoustic-elastic coupling considering finite elements and the acoustic-acoustic coupling considering finite elements and finite differences (other coupling procedures can be implemented analogously). One important feature of the algorithms presented is that they allow considering different time-steps for different sub-domains; so it is possible to substantially improve efficiency, accuracy and stability of the central difference time integration algorithm employed here. Three examples, presented at the end of the paper, show the excellent performance of the algorithms developed.

Keyword: Acoustics; Elastodynamics; Partitioned coupled systems; Finite elements; Finite differences; Multi-level time-steps; Marine risers.

1 Introduction

Time-domain finite difference modelling of wave propagation in highly heterogeneous media requires robust simulation algorithms in order to preserve accuracy, efficiency and stability (explicit time integration procedures, e.g., the central difference method, have strict stability re-

quirements). Discontinuity of physical properties, across arbitrary shaped interfaces, may lead to low-quality finite difference results. Lombard and Piraux (2004) list the following main reasons for low confidence results in the aforementioned situation: spurious diffractions occur due to the stair-step representation of arbitrary shaped interfaces [Collino et al. (1997)]; reduction of the convergence order due to the non-smoothness of the solution across the interfaces, leading to numerical instabilities even for low contrast of physical parameters [Zhang and LeVeque (1997)]; the jump conditions and the boundary conditions are not incorporated in the schemes, so that the conversion, refraction and diffraction wave phenomena are not correctly described [Lombard (2002)]. In addition to the aforementioned difficulties introduced by interfaces, efficiency is another issue that must be dealt with properly. Accuracy and stability may restrict the time-step size to small values, adequate to sub-domains with high wave propagation velocities; in this case, efficiency will be quite poor. This difficulty can be overcome in the case of heterogeneous media by subcycling techniques [Daniel (1997), Smolinski (1996), Belytschko and Lu (1993)], which allow adopting different time-steps for pre-established sub-domains; one such a technique is discussed here. Subcycling requires establishing adequate coupling conditions between sub-domains; this topic is addressed here as well.

There are many other situations for which division in sub-regions and subcycling can be employed, with the same advantages of the case of heterogeneous media. Some of these situations are listed below, including those concerning heterogeneous media discussed above:

¹ Civil Engineering Department, COPPE/UFRJ, CXP 68506, CEP 21945-970, Rio de Janeiro, RJ, Brazil. Emails: webe@coc.ufrj.br; delfim@coc.ufrj.br

² Structural Engineering Department, UFJF, Cidade Universitária, CEP 36036-330, Juiz de Fora, MG, Brazil.

³ Submarine Technology, CENPES/PETROBRAS, Ilha do Fundão, CEP 21949-900, Rio de Janeiro, RJ, Brazil.

- (a) Distinct physical properties;
- (b) Distinct media;
- (c) Distinct numerical methods;
- (d) Distinct behaviour (elastic/plastic; finite/infinity etc.);
- (e) Combination of (a), (b), (c), (d); etc.

The analysis of wave propagation in infinite domains is one case where the domain must be sub-divided at least into two sub-domains: a finite one and an unbounded one, the latter being responsible for propagating waves to infinity. There are many distinct approaches, generically referred to as transmitting boundaries, to represent unbounded sub-domains; usually, a numerical procedure, distinct from that of the bounded region is employed. Transmitting boundaries can employ very simple algorithms, as it is usual in RTM procedures in Geophysics, where it is quite common to employ a local transmitting boundary which consists simply of a rule to artificially reduce amplitude in an extended mesh [Bulcão (2005)]; on the other hand, very sophisticated approaches, such as boundary elements coupling, can be preferred [for a short review, see Soares Jr et al. (2004, 2005a-c) and Lie et al. (2001)].

It is described above a case where it is highly recommended to use partitioned analysis of a coupled system. Many other cases where it is advisable to use such a technique can be found in the literature, a review of some cases and procedures concerning the matter is described in the work of Park and Felippa [chapter 7 of Belytschko and Hughes (1983)].

In the present paper, the FEM (Finite Element Method) and the FDM (Finite Difference Method) are employed to establish time-domain computational algorithms to deal with the above described (a)-(e) item cases; acoustic and elastic wave propagations, as well as interacting acoustic-elastic waves are considered.

Standard fourth order in space / second order in time finite difference algorithms may become unstable in the case of heterogeneous acoustic media, specially in the presence of discontinuous

physical properties. Some finite difference based procedures have been developed to overcome this difficulty; e.g., the space and time fourth order scheme by Cohen and Jolly (1990). The alternative adopted here, to keep low costs (and stability), is to consider acoustic-acoustic coupling, employing finite elements to model the heterogeneous region and finite differences to model the remainder. Enhanced stability, efficiency and accuracy can be achieved by applying different time-steps for each sub-domain.

It is important to notice that the literature reports many stable FE procedures to deal with time integration of hyperbolic equations governing wave propagation. For a review up to the 80's, see Belytschko and Hughes (1983); for updated review, see Tamma et al. (2000) and for stabilized procedures see Hulbert and Hughes (1990).

The developments presented here apply to model the propagation of interacting acoustic-elastic waves. A finite difference based scheme that was successfully developed to deal with this problem is that presented by Lombard and Piraux (2004), which requires the solution of SVD (singular value decomposition) problems in order to properly compute interfaces variables. Another possible finite difference alternative approach to deal with this very same problem is that proposed by Virieux (1986), improved later on by Levander (1988). These two last procedures are very successful in applications concerning geophysics; but have not yet been tested in applications such as that presented here.

The alternative procedure, proposed by the present work, focus on acoustic-elastic coupling by FEM and acoustic-acoustic coupling by FEM and FDM. Thus, it employs well-known numerical procedures and it maintains the original hyperbolic system of equations, so boundary and interface conditions, as well as other problem variables, are those familiar to engineers, physicists etc..

The idea of coupling the FEM and the FDM (adopted here in order to take advantage of the low CPU cost of the latter) can be found in previous works, as for instance in Xing et al. (2003) and Chen (1998), who developed procedures for

fluid-structure interaction to compute hydrodynamic pressures and structural responses. However, partitioned coupling algorithms similar to those employed here are not known by the authors.

The use of adequate coupling conditions between sub-domains and the correct choice of the proper time-step for each sub-domain lead to stable, efficient and accurate procedures.

2 Governing Equations

In the present section, acoustic and elastic wave equations are briefly presented. Each one of these wave propagation models is used to model different sub-domains of the global problem. At the end of the section, basic equations concerning the coupling of acoustic and elastic sub-domains are described.

2.1 Acoustic Sub-Domains

The scalar wave equation is given by

$$(Kp_{,i})_{,i} - \rho\ddot{p} - \xi\dot{p} + S = 0 \quad (1)$$

where $p(X, t)$ stands for hydrodynamic pressure distribution and $S(X, t)$ for body source terms. Inferior commas (indicial notation is adopted) and over dots indicate partial space ($p_{,i} = \partial p / \partial x_i$) and time ($\dot{p} = \partial p / \partial t$) derivatives, respectively. $\xi(X)$ stands for the viscous damping coefficient; $\rho(X)$ is the mass density and $K(X)$ is the bulk modulus of the medium. In homogeneous media, ρ and K are constant and the classical wave equation (disregarding damping) can be written as

$$p_{,ii} - \ddot{p}/c^2 + s = 0 \quad (2)$$

where $c = \sqrt{K/\rho}$ is the wave propagation velocity. The boundary and initial conditions of the problem are given by

(i) Boundary conditions ($t > 0, X \in \Gamma$ where $\Gamma = \Gamma_1 \cup \Gamma_2$):

$$p(X, t) = \bar{p}(X, t) \quad \text{for } X \in \Gamma_1 \quad (3a)$$

$$q(X, t) = p_{,j}(X, t)n_j(X) = \bar{q}(X, t) \quad \text{for } X \in \Gamma_2 \quad (3b)$$

(ii) Initial conditions ($t = 0, X \in \Gamma \cup \Omega$):

$$p(X, 0) = \bar{p}_0(X) \quad (4a)$$

$$\dot{p}(X, 0) = \dot{\bar{p}}_0(X) \quad (4b)$$

where the prescribed values are indicated by over bars and q represents the flux along the boundary whose unit outward normal vector components are represented by n_j . The boundary of the model is denoted by Γ ($\Gamma_1 \cup \Gamma_2 = \Gamma$ and $\Gamma_1 \cap \Gamma_2 = 0$) and the domain by Ω .

2.2 Elastic Sub-Domains

The elastic wave equation for homogenous media is given by

$$(c_d^2 - c_s^2)u_{j,ji} + c_s^2 u_{i,jj} - \ddot{u}_i - \zeta \dot{u}_i + b_i = 0 \quad (5)$$

where u_i and b_i stand for the displacement and the body force distribution components, respectively. The notation for time and space derivatives employed in equation (1) is once again adopted. In equation (5), c_d is the dilatational wave velocity and c_s is the shear wave velocity, they are given by: $c_d^2 = (\lambda + 2\mu)/\rho$ and $c_s^2 = \mu/\rho$, where ρ is the mass density and λ and μ are the Lamé's constants. ζ stands for viscous damping related parameters. Equation (5) can be obtained from the combination of the following basic mechanical equations (proper to model heterogeneous media)

$$\sigma_{ij,j} - \rho\ddot{u}_i - \rho\zeta\dot{u}_i + \rho b_i = 0 \quad (6a)$$

$$\sigma_{ij} = \lambda \delta_{ij} \varepsilon_{kk} + 2\mu \varepsilon_{ij} \quad (6b)$$

$$\varepsilon_{ij} = (u_{i,j} + u_{j,i})/2 \quad (6c)$$

where σ_{ij} and ε_{ij} are, respectively, stress and strain tensor components and δ_{ij} is the Kronecker delta ($\delta_{ij} = 1$, for $i = j$ and $\delta_{ij} = 0$, for $i \neq j$). Equation (6a) is the momentum equilibrium equation; equation (6b) represents the constitutive law of the model and equation (6c) stands for kinematical relations. The boundary and initial conditions of the elastodynamic problem are given by

(i) Boundary conditions ($t > 0, X \in \Gamma$ where $\Gamma = \Gamma_1 \cup \Gamma_2$):

$$u_i(X, t) = \bar{u}_i(X, t) \quad \text{for } X \in \Gamma_1 \quad (7a)$$

$$\tau_i(X, t) = \sigma_{ij}(X, t) n_j(X) = \bar{\tau}_i(X, t) \quad \text{for } X \in \Gamma_2 \quad (7b)$$

(ii) Initial conditions ($t = 0, X \in \Gamma \cup \Omega$):

$$u_i(X, 0) = \bar{u}_{i0}(X) \quad (8a)$$

$$\dot{u}_i(X, 0) = \dot{\bar{u}}_{i0}(X) \quad (8b)$$

where the prescribed values are indicated by over bars and τ_i denotes the traction vector along the boundary (n_j , as indicated previously, stands for the components of the unit outward normal vector).

2.3 Acoustic-Elastic Interacting Interfaces

On the acoustic-elastic interface boundaries, the elastic sub-domain normal (normal to the interface) accelerations (\ddot{u}_n) are related to the acoustic sub-domain fluxes (q), and the acoustic sub-domain hydrodynamic pressures (p) are related to the elastic sub-domain normal tractions (τ_n). These relations are expressed by the following equations

$$\ddot{u}_n - (1/\rho)q = 0 \quad (9a)$$

$$\tau_n + p = 0 \quad (9b)$$

where equations (9) takes into account that outward normal vectors at the same interface point are opposite for adjacent sub-domains. In equation (9a), ρ is the mass density of the interacting acoustic sub-domain medium.

3 Numerical Modelling

In the present section, numerical discretization by finite element and finite difference methods is briefly discussed and coupling procedures are presented.

Each sub-domain of the global model is solved independently in the present work, using standard finite element and finite difference techniques. The central difference time-marching scheme (explicit solution) is considered for all sub-domains (different time-steps in each sub-domain may be considered). The coupling of different sub-domains is directly taken into account, based on interacting interface values. As a consequence, an efficient and accurate explicit partitioned coupled algorithm is achieved.

3.1 Finite Element/Finite Difference Discretization

After space discretization either by finite elements or by finite differences, the following system of equations is obtained (in matrix form)

$$\mathbf{M}\ddot{\mathbf{X}}^t + \mathbf{C}\dot{\mathbf{X}}^t + \mathbf{K}\mathbf{X}^t = \mathbf{F}^t \quad (10)$$

where \mathbf{M} , \mathbf{C} and \mathbf{K} are mass, damping and stiffness matrices, respectively. Equation (10) is a general representation expression: one should note that different mass, damping and stiffness matrices are involved, however, according to the different formulations (acoustic/elastic) and numerical techniques (FEM/FDM) employed. In the present work, diagonal mass and damping matrices are adopted. Although, in the FDM, diagonal mass and damping matrices appear naturally; in the FEM, lumped matrix formulations must be employed. In equation (10), \mathbf{X}^t is the pressure/displacement vector (acoustic/elastic formulation, respectively) of the FEM/FDM assemblage, at time t . \mathbf{F}^t is the vector of generalized applied loads.

After applying the central difference scheme to integrate equation (10) in time, adopting a Δt time-step, the following system of equations is obtained

$$\mathbf{X}^{t+\Delta t} = \mathbf{A}^{-1} \left\{ \mathbf{F}^t - (\mathbf{K} - (2/\Delta t^2)\mathbf{M}) \mathbf{X}^t - ((1/\Delta t^2)\mathbf{M} - (1/(2\Delta t))\mathbf{C}) \mathbf{X}^{t-\Delta t} \right\} \quad (11)$$

where $\mathbf{A} = (1/\Delta t^2)\mathbf{M} + (1/(2\Delta t))\mathbf{C}$. Therefore, as one can observe, if the mass and damping matrices are diagonal, the system of equations (11) can be explicitly solved (without factorizing a matrix etc.); i.e., only simple matrix multiplications are required, which can be evaluated at the element (FEM) or grid point (FDM) level. Once the vector $\mathbf{X}^{t+\Delta t}$ is evaluated, its time derivatives may be obtained, if necessary, by

$$\dot{\mathbf{X}}^t = (\mathbf{X}^{t+\Delta t} - \mathbf{X}^{t-\Delta t}) / (2\Delta t) \quad (12a)$$

$$\ddot{\mathbf{X}}^t = (\mathbf{X}^{t+\Delta t} - 2\mathbf{X}^t + \mathbf{X}^{t-\Delta t}) / (\Delta t^2) \quad (12b)$$

Further details concerning finite element and finite difference discretizations, as well as the central

difference time-integration scheme, can be found in Bathe (1996), Hughes (2000), Zienkiewicz and Taylor (2000), Ritchmeyer and Morton (1967), Alford et al. (1974), Cohen and Jolly (1990) etc..

3.2 Coupling Procedures

Acoustic-elastic, acoustic-acoustic and elastic-elastic coupling are considered in the present work; however, the focus here is on the acoustic-elastic coupling considering finite elements, and on the acoustic-acoustic coupling considering finite elements and finite differences (the other coupling procedures can be implemented analogously).

The coupling algorithm presented here takes advantage of the FEM and the FDM favourable characteristics, in order to develop an efficient final algorithm. The following characteristic of these numerical methods are explored: (i) the flexibility of the FEM to consider non-structured meshes, heterogeneous media etc.; (ii) the efficiency of the FDM, generating low CPU demanding codes.

The FDM is very effective to deal with acoustic wave propagation in homogenous media, a characteristic that is fully explored here; the FEM is employed here to discretize elastic bodies and acoustic media in its neighbourhood, so that it becomes possible to take full advantage of the FEM favourable features to consider irregular geometries and non-homogeneous physical property distributions. Therefore, in the present work, only finite elements procedures are employed to model elastic media; however, the basic concepts here presented can also be used if one wishes to employ FDM to model elastodynamic problems. In fact, the range of combinations is quite extensive.

Firstly, in the present sub-section, a coupling procedure for acoustic and elastic media is discussed, taking into account finite elements procedures. Then, procedures for coupling acoustic-acoustic and elastic-elastic media, adopting the FEM and the FDM is presented. Finally, at the end of the sub-section, time interpolation procedures are described, which allow considering different time-steps in each sub-domain of the global model. The choice of the appropriate time-step for each

sub-domain is very important here, to achieve efficiency, accuracy and stability (one should keep in mind that the central difference time integration method is conditionally stable).

3.2.1 Acoustic-Elastic Coupling

As it was mentioned previously, each sub-domain of the global model is solved independently in the present work, using standard finite element and finite difference techniques. For the acoustic-elastic coupling, taking into account finite element procedures, equation (11) is applied independently to the acoustic and elastic sub-domains, evaluating the respectively related vectors $\mathbf{X}_p^{t+\Delta t}$ and $\mathbf{X}_u^{t+\Delta t}$.

The coupling of these sub-domains at the current time is achieved through previous time-step forces, which are evaluated using interface values, as established by equations (9). The previous time-step interacting forces (\mathbf{R}^t) are introduced in the global force vector (\mathbf{F}^t). Once each \mathbf{F}^t vector is properly established, equation (11) can be simply evaluated within each sub-domain, keeping the systems of equations explicit and independent.

The interacting interface forces (\mathbf{R}^t) are given, at element level, by

$$\mathbf{R}_u^t = \left(\int_{\Gamma_I} \mathbf{N}_u^T \mathbf{n} \mathbf{N}_p d\Gamma \right) \mathbf{X}_p^t = \mathbf{Q} \mathbf{X}_p^t \quad (13a)$$

$$\mathbf{R}_p^t = - \left(\int_{\Gamma_I} \rho \mathbf{N}_p^T \mathbf{n}^T \mathbf{N}_u d\Gamma \right) \ddot{\mathbf{X}}_u^t = -\rho \mathbf{Q}^T \ddot{\mathbf{X}}_u^t \quad (13b)$$

where equations (13) are based on finite element procedures and on equations (9). In these equations, \mathbf{N}_p and \mathbf{N}_u are appropriate finite element shape functions; \mathbf{n} is the normal unit outward vector to the interface (Γ_I); ρ is the mass density of the interacting acoustic sub-domain medium (it is assumed constant within each element, so it is not included in the final integrand of equation (13b)); and \mathbf{Q} is the coupling matrix.

One should observe that equations (13) only employ previous discrete time values (\mathbf{X}_p^t and $\ddot{\mathbf{X}}_u^t$): equation (11) can then be directly employed, once all right-hand-side terms are known, for each

time-step. Care must be taken once $\ddot{\mathbf{X}}_u^t$ is being considered (equation (13b)). As expressed by equation (12b), acceleration vectors are evaluated at time t , whereas displacements are evaluated at time $t + \Delta t$. So, all elastic sub-domains should be analyzed first, generating all necessary information ($\ddot{\mathbf{X}}_u^t$, and as a consequence \mathbf{R}_p^t and \mathbf{F}_p^t) to obtain the solution of acoustic sub-domains.

3.2.2 Acoustic-Acoustic/Elastic-Elastic Coupling

For the acoustic-elastic coupling algorithm previously presented, the basic idea was to solve the system of equations of each sub-domain separately, applying natural boundary conditions on the interacting interfaces. The system of equations of each sub-domain is still to be solved separately for the coupling algorithms of the present sub-section; however, essential boundary conditions are considered on the interacting interfaces.

The basic idea here is to superpose interacting meshes (FEM or FDM meshes) and use internal nodal results of one sub-domain, as essential boundary conditions for the other interacting sub-domain, and vice-versa. This procedure will be explained taking into account acoustic-acoustic coupling using finite element and finite difference procedures. The other combination algorithms are analogous.

In Fig.1 a sketch for the acoustic-acoustic coupling of a linear quadrilateral FEM mesh and a fourth order FDM mesh is depicted. The meshes are superposed at the gray background selected nodes. Each sub-domain is solved separately, employing equation (11). On the interacting region (gray nodes in Fig.1), previous results from one sub-domain are applied as prescribed values for the other sub-domain, and unknowns for this last sub-domain are computed by direct use of equation (11). The solution for each sub-domain is obtained independently for each time-step, once only previous discrete time related prescribed values are necessary. In the Fig.1 illustration, for instance, the FDM results can be evaluated at the grid points (open circle and open circle with gray square background), using for each time-step the values of the FEM sub-domain at the grid points

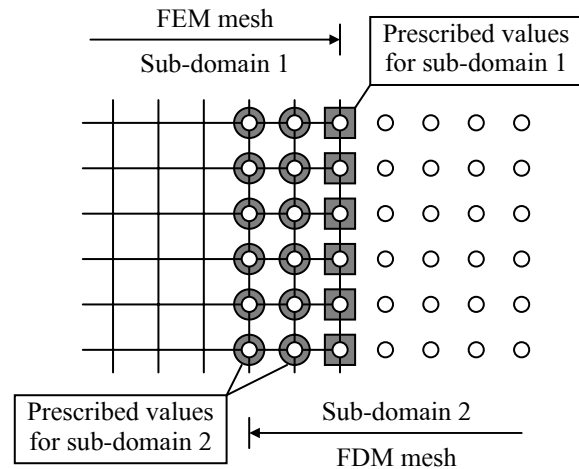


Figure 1: Acoustic-acoustic coupling of a linear quadrilateral FEM mesh and a fourth order FDM mesh: superposed meshes and sub-domains prescribed essential values.

with gray circle background. The FEM results, on the other hand, can be evaluated at the mesh nodes, using for each time-step the values of the FDM sub-domain at the mesh nodes with grey square background.

For coupled linear FEM-FEM meshes (acoustic-acoustic or elastic-elastic), or for coupled linear FEM mesh and second order FDM mesh, the same basic concept can be employed. The interface region, however, is simpler, being necessary just one layer of gray circle background nodes. The concept is also analogous for quadratic, cubic etc. FEM meshes.

3.2.3 Different Time-Steps

The central difference time integration method is conditionally stable; therefore, an appropriate time-step selection within each sub-domain is extremely important. The present approach permits using different time-steps for each sub-domain, producing a more stable, accurate and efficient algorithm.

Each sub-domain is considered separately as specified by equation (11), interactions among the different sub-domains being enforced by means of natural or essential boundary conditions, as dis-

cussed above. These coupling boundary conditions can be time interpolated, allowing different time discretizations to be employed for each sub-domain. Fig. 2 shows a linear time-interpolation

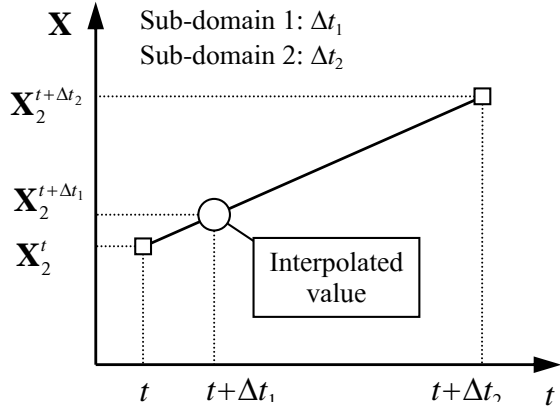


Figure 2: Linear time-interpolation procedure: interpolation of sub-domain 2 interacting values for application as prescribed boundary condition (natural or essential) for sub-domain 1.

sketch in order to illustrate the interaction of two hypothetical sub-domains: sub-domain 1, with time-step Δt_1 , and sub-domain 2, with time-step Δt_2 . It is considered that $\Delta t_2 = m\Delta t_1$, where m is a natural number. Equations for sub-domain 1 are then solved m times within the time-step of sub-domain 2. The boundary values necessary to obtain the sub-domain 1 solution, at each one of these m time instants, are obtained from time-interpolated values of sub-domain 2. Fig.2 depicts the linear time-interpolation sketch for the interacting values of sub-domain 2.

4 Numerical Applications

Three applications of the previously presented procedures are discussed in this section. In the first application, a simple “theoretical” three-dimensional problem is focused on: several combinations of the coupling procedures are considered and the results obtained are compared with a standard FEM solution. In the second application, an axisymmetric approach is adopted to model the propagation of waves through the steel wall

of a submerged marine riser, the results achieved being compared with experimental data. The third application, once again concerns the study of wave propagation through marine risers (to be more specific: two marine risers, one inside the other), this time, a bi-dimensional model is adopted.

4.1 Three-Dimensional Application

In this sub-section, a three-dimensional column is analysed. A sketch of the problem is depicted in Fig.3(a). The geometrical dimensions of the column are: $10m \times 10m \times 50m$. Two media (of equal length and cross section) compose the column; the physical properties of each medium are (null Poisson rate is adopted for elastodynamic sub-domains):

- Medium 1: $\rho_1 = 1 \text{ kg/m}^3$ (mass density) and $c_1 = 10 \text{ m/s}$ (wave velocity)
- Medium 2: $\rho_2 = 1 \text{ kg/m}^3$ (mass density) and $c_2 = 5 \text{ m/s}$ (wave velocity)

Three different numerical models are considered to simulate this problem, taking into account different coupling procedure combinations. A sketch of the three models adopted is presented in Fig.3(b). Details about each numerical model are given below:

- Model 1: elastodynamic FEM formulations are employed. Two independent FEM meshes are adopted, the first one with 2600 linear hexahedral elements and the other one with 2500 linear hexahedral elements (100 elements, i.e., one “element layer”, are used for mesh superposition).
- Model 2: elastodynamic and acoustic FEM formulations are employed, as well as acoustic FDM formulation. 2500 linear hexahedral elements are adopted for the FEM elastodynamic mesh and 1000 linear hexahedral elements are adopted for the FEM acoustic mesh. 2178 grid points are employed by the space fourth-order FDM discretization (grid points for mesh superposition included).

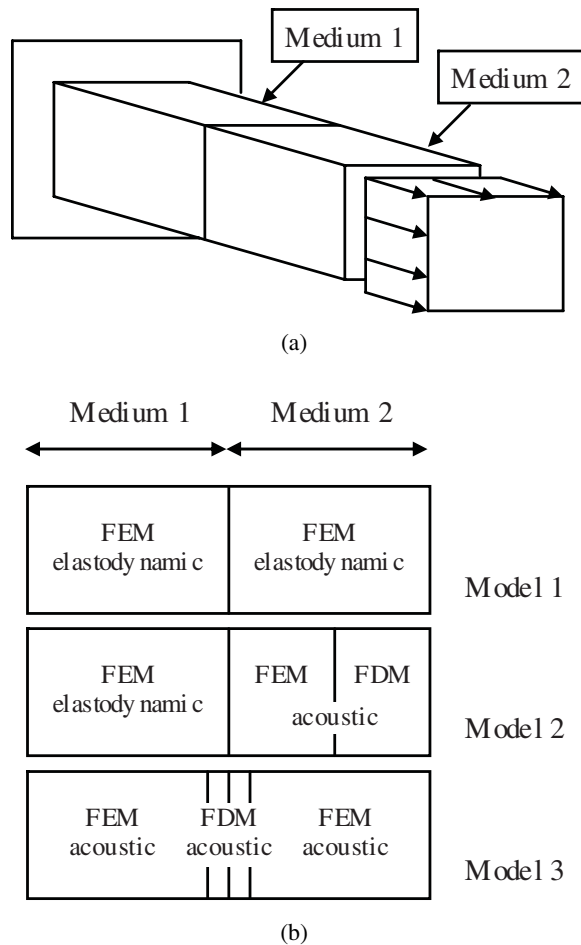


Figure 3: Three-dimensional application: (a) sketch of the physical problem; (b) sketch of the models used to obtain numerical solutions.

- Model 3: acoustic FEM and FDM formulations are employed. Two independent FEM meshes are adopted, each one with 2000 linear hexahedral elements. 1815 grid points are employed by the space fourth-order FDM discretization (grid points for mesh superposition included).

Two numerical analyses were considered, namely: (a) homogeneous analysis, where the entire column is considered composed by medium 1; (b) heterogeneous analysis, where half of the column is considered composed by medium 1, and the other half by medium 2. The results achieved for the three different numerical models described above are depicted in Fig.4. The

heterogeneous analysis considered two different time-steps, namely: $\Delta t_1 = 0.05 s$ (medium 1) and $\Delta t_2 = 0.10 s$ (medium 2). For the homogeneous analysis $\Delta t = 0.05 s$ was adopted for the entire domain. In Fig.4, reference results are also depicted: these results correspond to a standard FEM simulation with 5000 linear hexahedral elements and $\Delta t = 0.05 s$ (homogeneous and heterogeneous analyses). As one can see, results for all simulations are in good agreement.

In the present heterogeneous analysis, for instance, the advantages of the proposed procedures may be highlighted under several aspects: different time-steps are easily adopted for each sub-domain, as a consequence the algorithm becomes quite robust even when considering media with high properties contrast and less systems of equations need to be solved along the time-marching process; not all sub-domains need to be considered at initial time-steps, the activation/initialisation of different sub-domains may be controlled based on the properties of the model (wave propagation velocities etc.), saving most of the computational effort of the first time-steps etc..

4.2 Axissimetric Application

In the present sub-section, the wave propagation through the steel wall of a submerged marine riser is studied. An axissimetric numerical model is adopted to simulate the problem. A sketch of the model is depicted in Fig.5(a). In the present application, most of the domain is modelled by the FDM acoustic formulation (water). The metallic tube wall (marine riser) is modelled by the FEM elastodynamic formulation. A thin water layer surrounding the tube wall is also modelled by the FEM (acoustic formulation).

Two different modelling procedures were adopted to simulate the source: (a) the source was considered punctual and an excitation term was introduced in the correspondent grid point of the FDM mesh; (b) the source was considered spherical (radius $0.03429 m$), and a FEM mesh was introduced to properly model its neighbourhood (this mesh is depicted in Fig.5(b)).

Results obtained from a laboratory experiment

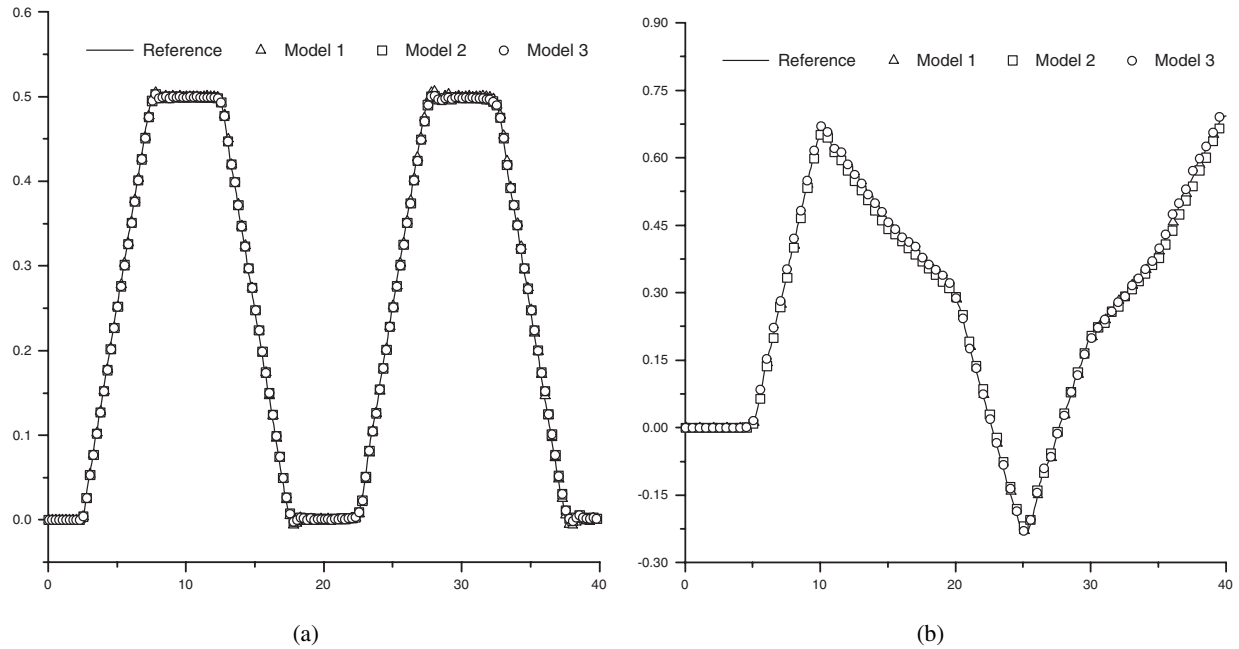


Figure 4: Numerical solution of the three-dimensional application (displacement/pressure x time) at the interface: (a) homogeneous analysis; (b) heterogeneous analysis.

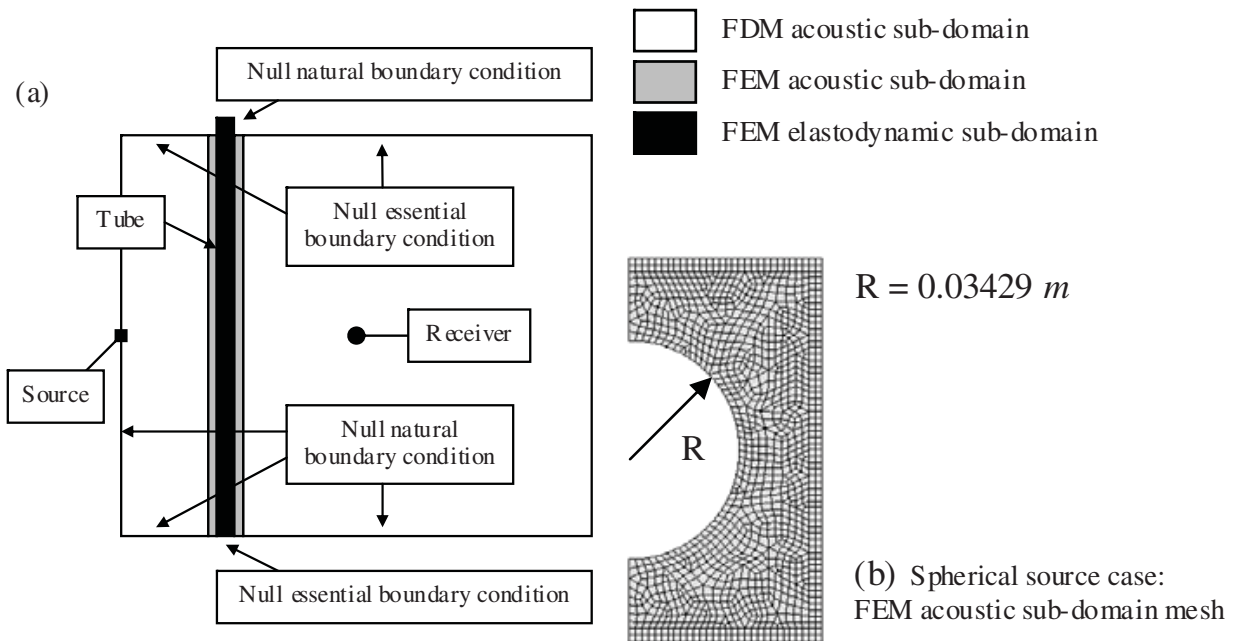


Figure 5: Axissymmetric application: (a) sketch of the numerical model; (b) detail of the FEM mesh adopted to model the neighbourhood of the spherical source.

[Lima (2004)], as illustrated in Fig.6, were used to validate the numerical response.

The properties of the related media are given be-

low:

- Water: $c = 1500 \text{ m/s}$ (sound velocity); $\rho = 1030 \text{ kg/m}^3$ (mass density).

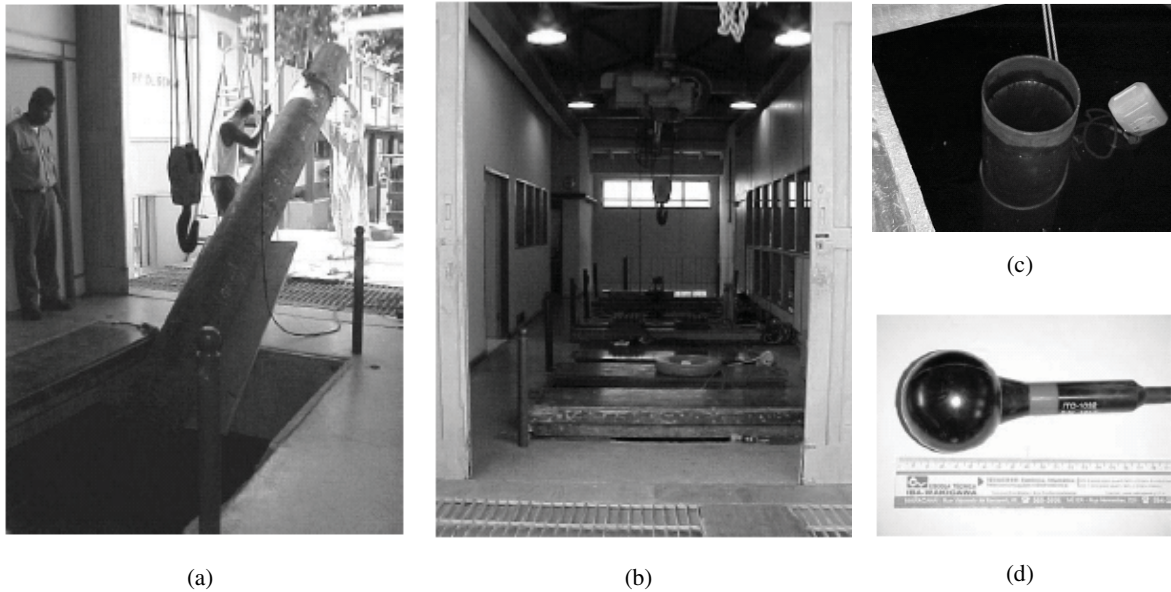


Figure 6: Photos of the experiment: (a) tube installation through the water tank input gate; (b) tank facilities; (c) tube inside the tank (view through the gate); (d) acoustic transducer ITC 1032 (source/receptor).

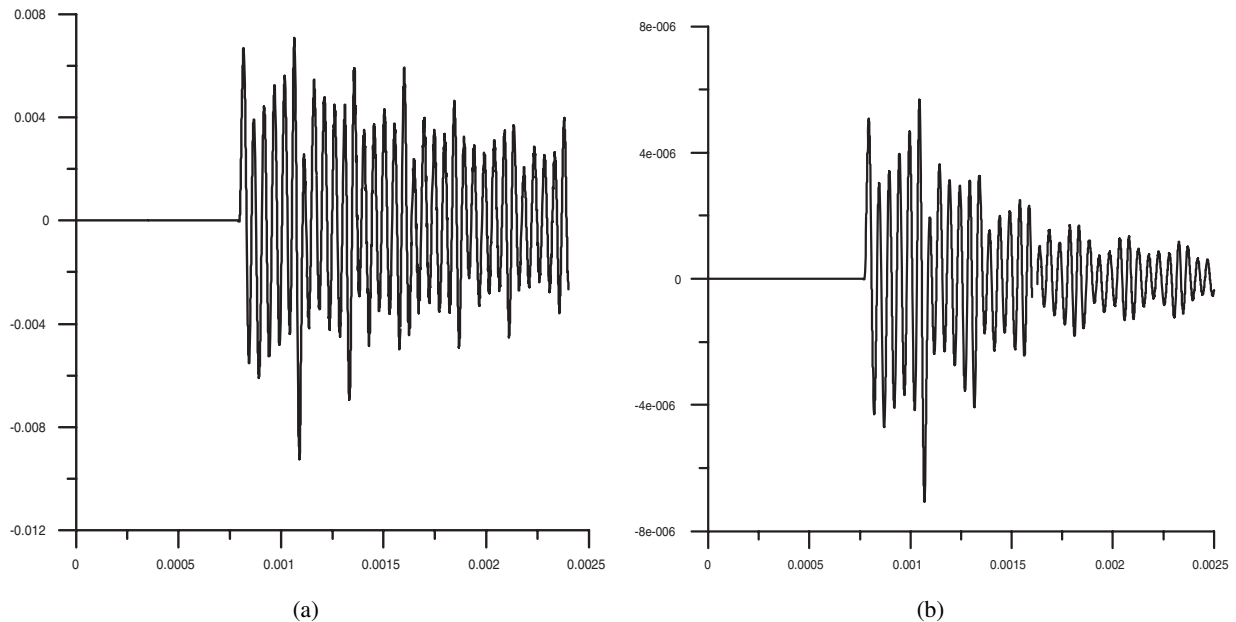


Figure 7: Numerical solution of the axisymmetric application (pressure x time) at the receiver : (a) punctual source case; (b) spherical source case.

- Tube: $\phi = 410 \text{ mm}$ (external diameter); $t = 12 \text{ mm}$ (thickness); $h = 4.7 \text{ m}$ (height); $E = 2.1 \cdot 10^5 \text{ MPa}$ (Young modulus); $\nu = 0.3$ (Poisson rate); $\rho = 7700 \text{ kg/m}^3$ (mass density).

The source produces a sinusoidal excitation with

frequency of 20 kHz and duration of $3.0 \cdot 10^{-4} \text{ s}$. The time-steps adopted, for each sub-domain, for the numerical modelling were: $\Delta t_1 = 2.0 \cdot 10^{-7} \text{ s}$ (FDM mesh and FEM spherical source mesh); $\Delta t_2 = 1.0 \cdot 10^{-7} \text{ s}$ (FEM mesh surrounding the tube wall) and $\Delta t_3 = 0.5 \cdot 10^{-7} \text{ s}$ (FEM tube mesh).

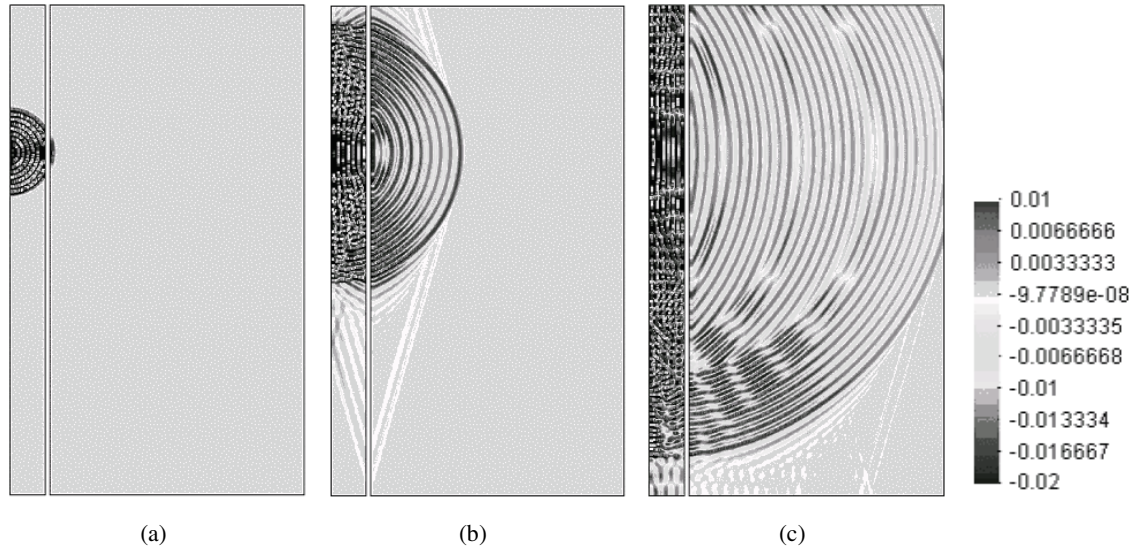


Figure 9: Pressure distribution for the punctual source case at three different moments: (a) begin of propagation; (b) wave fronts due to the faster propagation through the tube wall (head waves); (c) reinforcement of amplitude.

The results achieved for the hydrodynamic pressure at the receiver (hydrophone) are depicted in Fig.7(a) and Fig.7(b), for the punctual and spherical source cases, respectively. The results obtained by the experimental model are depicted in Fig.8. As one can observe, good agreement between experimental and numerical (spherical source case) simulations has been obtained (the scale of the graphics should be ignored, since the source intensities adopted in each analysis are different). Comparing the results depicted in Fig.7(a) and in Fig.7(b), one can clearly observe the energy dissipation in the source-receiver direction, due to the scattering induced by the spherical source. Fig.9 depicts three snapshots of the numerical analysis (punctual source case) and shows some interesting and important features related to the present wave propagation configuration, as for instance: wave fronts (head waves) arising from the faster propagation through the tube wall (Fig.9(b)) which generates a reinforcement of amplitude at the wave front region close to the tube. If one interprets the phenomenon thinking about rays (ray tracing theory), one may be led to erroneously think that there exists a reinforcement of the amplitude at oblique incidence (Fig.9(c)).

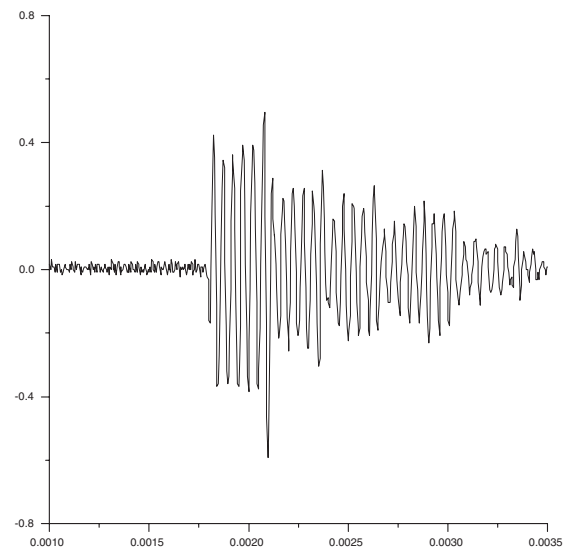


Figure 8: Experimental results (pressure x time) at the receiver.

4.3 Bi-Dimensional Application

The study of wave propagation through marine risers is further explored in this third application. As depicted in the sketch shown in Fig.10, in the present sub-section two marine risers are analysed, one inside the other.

The two tubes are geometrically defined by (the

water and steel physical properties are the same as presented in sub-section 4.2):

- Tube 1: $\phi = 5\frac{1}{4}$ "(internal diameter); $t = \frac{1}{2}$ "(thickness)
- Tube 2: $\phi = 500\text{ mm}$ (external diameter); $t = 16\text{ mm}$ (thickness)

Six different sub-domains were adopted to numerically model the present configuration. Each sub-domain is described bellow:

- Sub-domain 1: water inside tube 1; acoustic FEM formulation mesh composed of 4989 quadrilateral linear elements; time-step equal to $5.0 \cdot 10^{-8}s$.
- Sub-domain 2: water inside tube 2 and outside tube 1; acoustic FEM formulation mesh composed of 48902 quadrilateral linear elements; time-step equal to $5.0 \cdot 10^{-8}s$.
- Sub-domain 3: water outside tube 2; acoustic FEM formulation mesh composed of 66294 quadrilateral linear elements; time-step equal to $10.0 \cdot 10^{-8}s$.
- Sub-domain 4: water outside FEM meshes; acoustic FDM formulation with 573049 grid points (fourth-order space discretization); time-step equal to $40.0 \cdot 10^{-8}s$.
- Sub-domain 5: tube 1; elastodynamic FEM formulation mesh composed of 3765 quadrilateral linear elements; time-step equal equal to $2.5 \cdot 10^{-8}s$.
- Sub-domain 6: tube 2; elastodynamic FEM formulation mesh composed of 13316 quadrilateral linear elements; time-step equal to $2.5 \cdot 10^{-8}s$.

The size of the finite elements of sub-domain 3 is continuously and slightly enlarged (from the connection to sub-domain 6 till the connection to sub-domain 4) in a way that a regular sufficiently large FDM mesh can be adopted (sub-domain 4) in order to represent the infinite medium.

The line source (2D source point), which is located at the centre of tube 2, produces a sinusoidal excitation with frequency of 30 kHz and duration of $3.0 \cdot 10^{-4}\text{ s}$.

The results achieved for the hydrodynamic pressure at the 6 receivers (see Fig.10) are depicted in Fig.11. Snap-shots of the hydrodynamic pressure results are presented in Fig.12, for three different time-instants and for the FEM acoustic sub-domains. The results illustrate quite well the interaction between the internal and the external marine risers as well as the propagation of waves within this complex configuration.

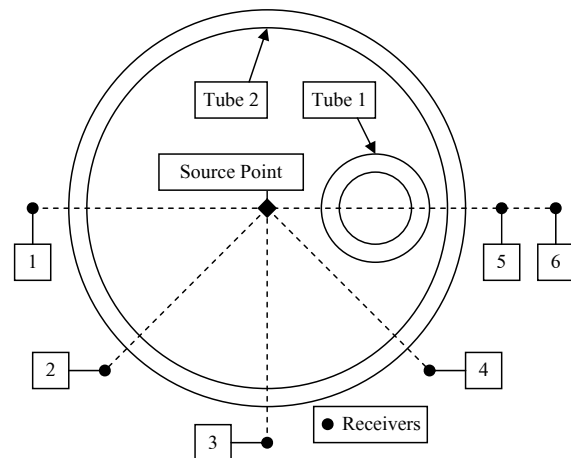


Figure 10: Bi-dimensional application: sketch of the physical problem.

5 Conclusions

The present paper presents an explicit multi-level time-step algorithm to model the propagation of interacting acoustic-elastic waves using finite element/finite difference coupled procedures.

The focus of the paper is the acoustic-elastic coupling considering finite elements and the acoustic-acoustic coupling considering finite elements and finite differences. The ideas presented can very easily be used for other combinations of methods and media. Coupling FE and FD methods permits to take advantage of the favourable characteristics of both methods leading to a stable and fast computational code. Efficiency and stability become possible once the procedure presented

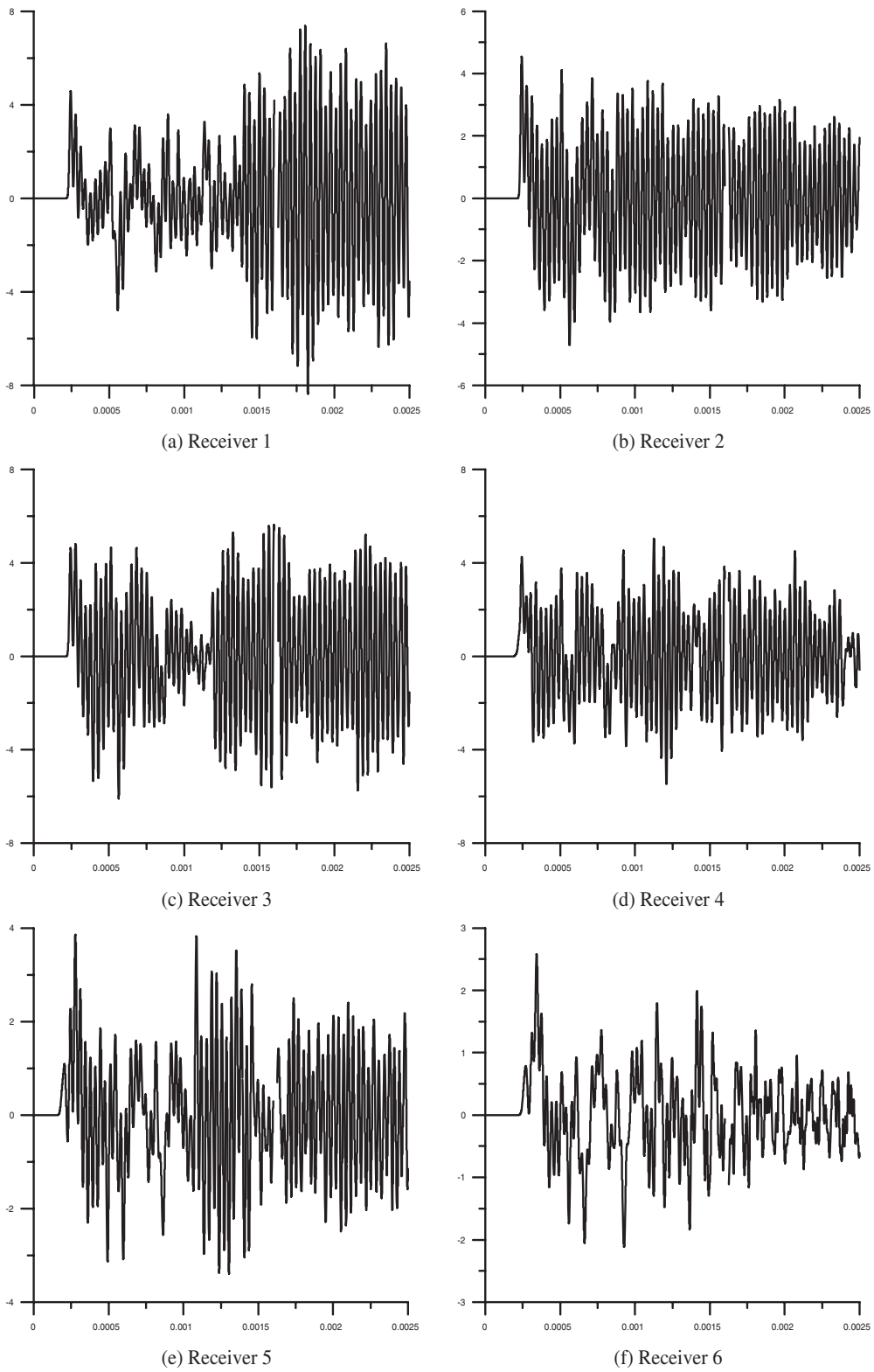


Figure 11: Numerical solution of the bi-dimensional application (pressure x time) at receivers.

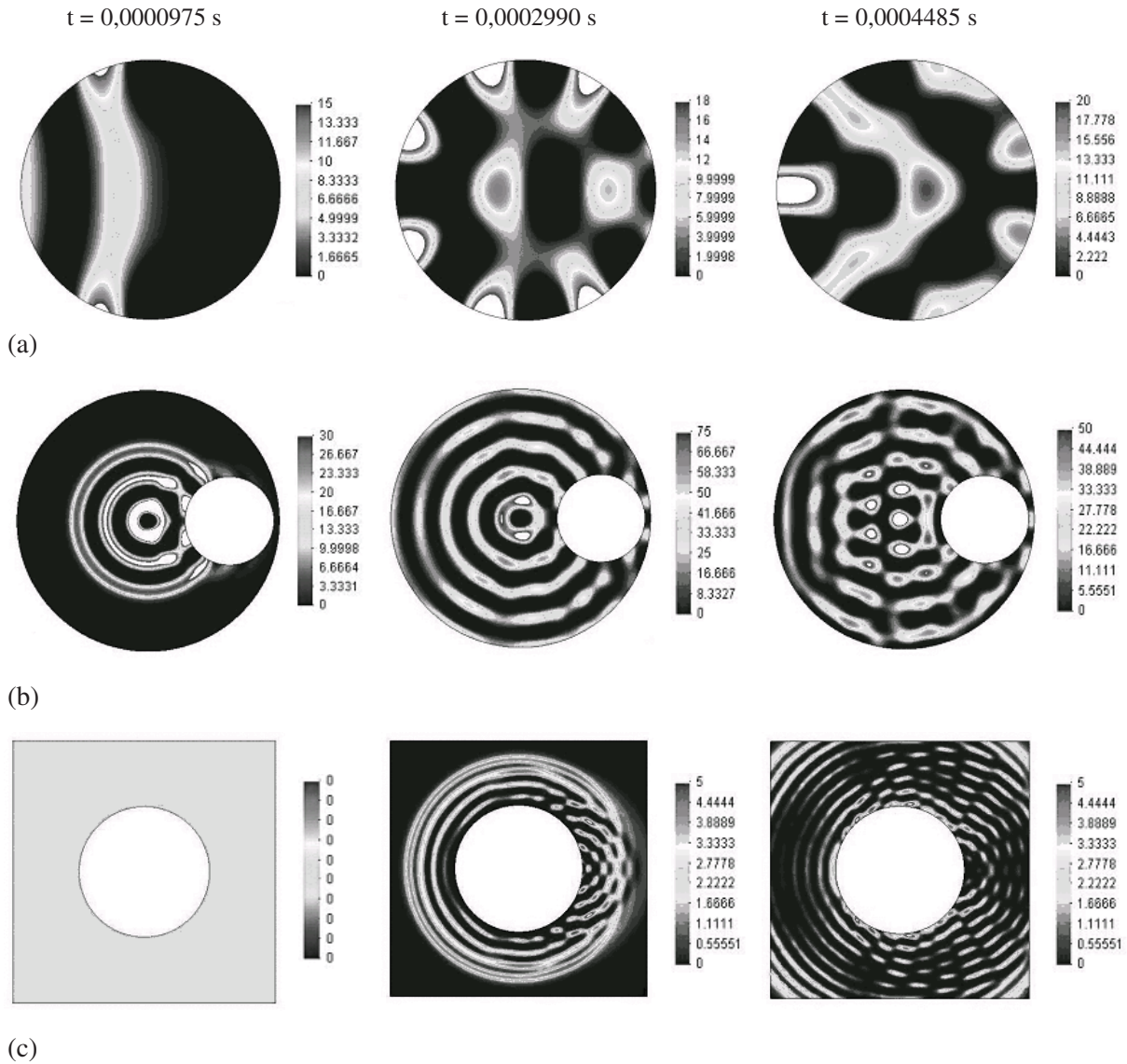


Figure 12: Pressure distribution along the FEM acoustic sub-domains at three different time-instants: (a) sub-domain 1; (b) sub-domain 2; (c) sub-domain 3.

permits the division of the heterogeneous media into sub-domains, allowing subcycling (i.e., allowing to employ adequate time-steps for each sub-domain considered).

Three examples were presented:

- The first example was used to validate the developed numerical algorithm. For a homogeneous and a heterogeneous three-

dimensional body, comparison of results obtained considering several numerical models and a standard reference solution showed that the developed algorithm gives quite accurate results;

- The second example employed an axisymmetric numerical model to study the wave propagation through a submerged marine riser.

Results obtained by the numerical simulation were compared with those obtained from a physical experiment. They were quite close as one can see comparing Figs. 7 and 8;

- The third example aimed at illustrating the application of the methodology to model a complex two-dimensional acoustic-elastic wave propagation configuration. It confirms the stability of the algorithm and its applicability to model acoustic signals through walls of marine risers.

Acknowledgement: The financial support by PETROBRAS (project number 0050.0011058.05.3) is greatly acknowledged, as well as the collaboration of engineers A. Warszawski and F. Brenny in the present project.

References

- Alford, R.M.; Kelly, K.R.; Boore, D.M.** (1974): Accuracy of finite difference modelling of the acoustic wave equation, *Geophysics*, vol. 39, pp. 834-842.
- Bathe, K.J.** (1996): *Finite element procedures*, 1 ed., Prentice Hall, New Jersey.
- Belytschko, T.; Hughes T.** (1983): *Computational Methods for Transient Analysis*, North-Holland, Amsterdam.
- Belytschko, T.; Lu, Y.Y.** (1993): Explicit multi-time step integration for first and second order finite element semi-discretization, *Computer Methods in Applied Mechanics and Engineering*, vol. 108, pp. 353-383.
- Bulcão, A.** (2005): Modeling and reverse time migration using elastic and acoustic operators, Ph.D. Thesis (in Portuguese), Federal University of Rio de Janeiro, Brazil.
- Chen, B.F.** (1998): Hybrid three-dimensional finite-difference and finite-element analysis of seismic wave induced fluid-structure interaction of a vertical cylinder, *Ocean Engineering*, vol. 25, pp. 639-656.
- Cohen, G.; Joly, P.** (1990): Fourth order schemes for the heterogeneous acoustic equation, *Computer Methods in Applied Mechanics and Engineering*, vol. 80, pp. 397-407.
- Collino, F.; Joly, P.; Millot F.** (1997): Fictitious domain method for unsteady problems: application to electromagnetic scattering, *Journal of Computational Physics*, vol. 138, pp. 907-938.
- Daniel, W.J.T.** (1997): Analysis and implementation of a new constant acceleration subcycling algorithm, *International Journal for Numerical Methods in Engineering*, vol. 40, pp. 2841-2855.
- Hughes, T.J.R.** (2000): *The finite element method - linear static and dynamic finite element analysis*, 2 ed., Prentice Hall, New Jersey.
- Hulbert, G.M.; Hughes, T.J.R.** (1990): Space-time finite element methods for second-order hyperbolic equations, *Computer Methods in Applied Mechanics and Engineering*, vol. 84, pp. 327-348.
- Levander, A.R.** (1988): Fourth-order finite-difference P-SV seismograms, *Geophysics*, vol. 53, pp. 1425-1436.
- Lie, S.T.; Yu, G. Y.; Zhao, Z.** (2001): Coupling of BEM/FEM for time domain structural-acoustic interaction problems, *CMES: Computer Modeling in Engineering & Sciences*, vol.2, pp. 171-180.
- Lima, D.L.** (2004): Through-riser acoustic communication system for ultra-deep water completion, M.Sc. Thesis (in Portuguese), Federal University of Rio de Janeiro, Brazil.
- Lombard, B.** (2002): Modélisation Numérique de la Propagation des Ondes Acoustiques et Élastiques en Présence d'Interfaces, Ph.D. Thesis, University of Aix-Marseille II, France.
- Lombard, B.; Piraux, J.** (2004): Numerical treatment of two-dimensional interfaces for acoustic and elastic waves, *Journal of Computational Physics*, vol. 195, pp. 90-116.
- Ritchmeyer, R.D.; Morton, K.W.** (1967): *Difference methods for initial value problems*, Interscience, New York.
- Smolinski, P.** (1996): Subcycling integration with non-integer time steps for structural dynamics problems, *Computers & Structures*, vol. 59, pp. 273-281.

Soares Jr, D.; Carrer, J.A.M.; Mansur, W.J. (2005a): Non-linear elastodynamic analysis by the BEM: an approach based on the iterative coupling of the D-BEM and TD-BEM formulations, *Engineering Analysis with Boundary Elements*, vol. 29, pp. 761-774.

Soares Jr, D.; Mansur, W.J. (2005b): An efficient time-domain BEM/FEM coupling for acoustic-elastodynamic interaction problems, *CMES: Computer Modeling in Engineering & Sciences*, vol.8, pp. 153-164.

Soares Jr, D.; von Estorff, O.; Mansur, W.J. (2004): Iterative coupling of BEM and FEM for nonlinear dynamic analyses, *Computational Mechanics*, vol. 34, pp. 67-73.

Soares Jr, D.; von Estorff, O.; Mansur, W.J. (2005c): Efficient nonlinear solid-fluid interaction analysis by an iterative BEM/FEM coupling, *International Journal for Numerical Methods in Engineering*, vol. 64, pp. 1416–1431.

Tamma, K.K.; Zhou X.; Sha D. (2000): The time dimension: a theory towards the evolution, classification, characterization and design of computational algorithms for transient/dynamic applications, *Archives of Computational Methods in Engineering*, vol. 7, pp. 67-290.

Virieux, J. (1986): P-SV wave propagation in heterogeneous media: velocity-stress finite difference method, *Geophysics*, vol. 51, pp. 889-901.

Xing, J.T.; Price, W.G.; Chen, Y.G. (2003): A mixed finite-element finite-difference method for nonlinear fluid-structure interaction dynamics - I. Fluid-rigid structure interaction, Proc. R. Soc. Lond. A., vol. 459, pp. 2399-2430.

Zhang, C.; LeVeque, R.J. (1997): The immersed interface method for acoustic wave equations with discontinuous coefficients, *Wave Motion*, vol. 25, pp. 237–263.

Zienkiewicz, O.C.; Taylor, R.L. (2000): *The finite element method*, 5th ed., Mc-Graw-Hill.